Inorganic Chemistry

Article

pubs.acs.org/IC

New Families of Hetero-tri-spin 2p−3d−4f Complexes: Synthesis, Crystal Structures, and Magnetic Properties

Lívia B. L. Escobar,[†] Guilherme P. Guedes,[§] Stéphane Soriano,[‡] Nivaldo L. Speziali,[⊥] Alessandro K. Jordão,[†] Anna Claudia Cunha,[†] Vitor F. Ferreira,[†] Catalin Maxim,[¶] Miguel A. Novak,[⊗] Marius Andruh,*[,¶] and Maria G. F. Vaz*[,†]

[†]Instituto de Química and [‡]Instituto de Física, Universidade Federal Fluminense, Niterói, Rio de Janeiro, Brazil

[§]Instituto de Ciências Exatas, Departamento de Química, Universidade Federal Rural do Rio de Janeiro, Seropédica, Rio de Janeiro, Brazil

[⊥]Departamento de Física, Universidade Federal de Minas Gerais, Belo Horizonte, Minas Gerais, Brazil

[¶]Inorganic Chemistry Laboratory, Faculty of Chemistry, University of Bucharest, Str. Dumbrava Rosie nr. 23, Bucharest, Romania

[⊗]Instituto de Física, Universidade Federal do Rio de Janeiro, Rio de Janeiro, Brazil

Supporting Information

ABSTRACT: In this work we report the synthesis, crystal structures, and magnetic behavior of 2p−3d−4f heterospin systems containing the nitroxide radical 4-azido-2,2,6,6-tetramethylpiperidine-1-oxyl radical (N_3tempo). These compounds were synthesized through a one-pot reaction by using [Cu(hfac)$_2$], [Ln(hfac)$_3$] (hfac = hexafluoroacetylacetonate, Ln = Dy^{III}, Tb^{III} or Gd^{III}), and the N_3tempo radical. Depending on the stoichiometric ratio used, the synthesis leads to penta- or trimetallic compounds, with molecular formulas [Cu_3Ln_2(hfac)$_8$(OH)$_4$(N_3tempo)] (Ln = Gd, Tb, Dy) and [$CuLn_2$(hfac)$_8$(N_3tempo)$_2$(H_2O)$_2$] (Ln = Gd, Dy). The magnetic properties of all compounds were investigated by direct current (dc) and alternating current (ac) measurements. The ac magnetic susceptibility measurements of Tb^{III}- and Dy^{III}-containing compounds of both families revealed slow relaxation of the magnetization, with magnetic quantum tunneling in zero field.

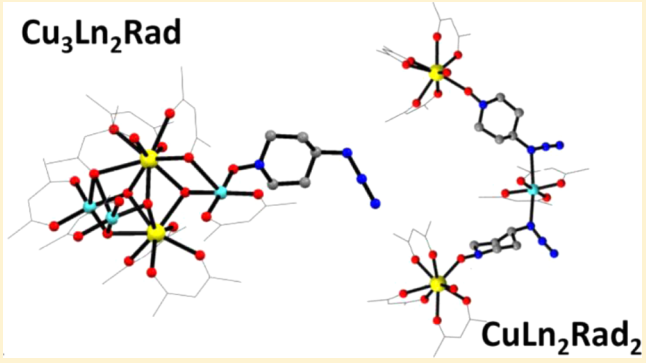

INTRODUCTION

The combination of different spin carriers within the same molecular entity is a broadly employed strategy to obtain molecular magnetic materials.[1,2] There are two main reasons for that: (i) the orthogonality of the magnetic orbitals of two different spin carriers, which leads to a ferromagnetic interaction, can be reached much more easily than the accidental orthogonality within the homospin systems, and (ii) even if the magnetic coupling is antiferromagnetic, the resulting spin can be big enough when a large spin (5/2, 7/2) interacts with a small one, such as a spin 1/2, for example. The ferrimagnetic approach to design molecule-based magnets, developed by Kahn and co-workers, is based on this last fact.[3] Indeed, one of the first rationally designed molecule-based magnets is a heterometallic coordination polymer containing Mn^{II} (S = 5/2) and Cu^{II} (S = 1/2).[4]

High-temperature molecular magnets are, in general, 3d−3d′ heterometallic coordination polymers.[5] The first report on the ferromagnetic interaction between Cu^{II} and Gd^{III}, made by Gatteschi et al.[6] and further observed with many other Cu^{II}−Gd^{III} complexes,[7] gave a strong impulse to the development of 3d−4f combined chemistry. From the magnetic point of view, the results were rather disappointing since the critical temperatures were extremely low. Recently, the 4f metal ions came back on the large stage of molecular magnetism after the characterization of the first single-molecule magnets (SMMs)[8] and single-chain magnets (SCMs) containing these ions.[9] Among the lanthanide cations, Tb^{III}, Dy^{III}, and Ho^{III}, which combine a large magnetic moment with a strong Ising-type magnetic anisotropy,[10] are especially used to obtain heterospin systems (3d−4f, 2p−4f, 4d−4f, 5d−4f) when looking for new SMMs and SCMs.

Numerous systems exhibiting interesting magnetic properties are based on the following pairs of spin carriers: 3d−4d,[11] 3d−5d,[11c,d,12] 3d−4f,[7,8a,13] 3d−5f,[14] 3d−Rad$^{\bullet}$,[15] 4f−Rad$^{\bullet}$,[16] 4f−

Received: April 9, 2014
Published: June 25, 2014

 © 2014 American Chemical Society dx.doi.org/10.1021/ic5008044 | Inorg. Chem. 2014, 53, 7508−7517

4d,[17] and 5d−4f.[18] In contrast, the number of polynuclear complexes containing three different spin carriers is much smaller. Various combinations can be imagined: 3d−3d′−3d″, 3d−3d′−4d, 3d−3d′−5d, 3d−3d′−Rad$^{\bullet}$, 3d−4f−Rad$^{\bullet}$, etc. Some of them are already illustrated by several compounds. The first trimetallic 3d−3d′−3d″ complexes, all metal ions being paramagnetic, were reported by Chaudhuri et al.[19] Their synthetic approach is based upon the use of bicompartmental ligands functionalized with oximato groups that coordinate to the third metal ion. A $[Cu^{II}Mn^{II}Cr^{III}]$ complex was obtained by assembling a preformed $[Cu^{II}Mn^{II}]$ complex with a bisoxalato−chromium complex that acts as a metalloligand.[20] A unique 3d−3d′−5d cluster, $[Fe^{II}_6Co^{II}_3W^{V}_6]$, was reported recently.[21] Several trimetallic complexes, containing lanthanide ions, 3d−3d′−4f, 3d−4d−4f, and 3d−5d−4f, have been also described.[22] Concerning the heterospin systems containing two different metal ions and an organic radical, the few known examples can be organized as follows: (i) supramolecular networks, constructed from heterobimetallic coordination polymers and uncoordinated/weakly coordinated radicals;[23] (ii) heterobimetallic 3d−3d′ complexes with the organic radicals acting as ligands;[24] (iii) heterobimetallic 3d−4f complexes with the organic radicals acting as ligands.[25] The first 2p−3d−4f and 3p−3d−4f complexes have been described by one of us[25a,26] and have been obtained by attaching the 2p ($TCNQ^{\bullet-}$) or 3p ($[Ni(mnt)_2]^{\bullet-}$) ligands to preformed $[Cu^{II}Ln^{III}Cu^{II}]$ complexes (TCNQ = 7,7,8,8-tetracyano-*p*-quinodimethane; mnt = maleonitriledithiolate). Unfortunately, in both cases the strong $\pi-\pi$ stacking interactions between the 2p or 3p spin carriers result in fully compensated antiferromagnetic pairs. Despite the intensive use of nitroxide and nitronyl nitroxide radicals since the early times of molecular magnetism, only very recently 2p−3d−4f coordination compounds, which were obtained by reacting hexafluoroacetylacetonates of Cu^{II} and Ln^{III} with nitronyl nitroxide radicals, have been reported.[25b,c] Herein we present our results concerning the synthesis, crystal structures, and magnetic behavior of two novel families of 2p−3d−4f discrete complexes, assembled using a tempo derivative as a ligand, namely, 4-azido-2,2,6,6-tetramethylpiperidine-1-oxyl (N_3tempo), shown in Chart 1. Although the spin density of the tempo detivative radicals is mainly located on the NO group,[15c] the functionalization of the four-position of the piperidinyl ring with the azide group gave rise to an additional coordination site, favoring the aggregation of the heterotrispin complexes.

Chart 1

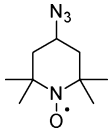

EXPERIMENTAL SECTION

Synthesis. All reagents and solvents were purchased from commercial sources and used without purification. The radical N_3tempo was prepared as described elsewhere.[27]

$[Cu_3Ln_2(hfac)_8(OH)_4(N_3tempo)]$. Ln = Gd^{III} (**1**), Tb^{III} (**2**), Dy^{III} (**3**): To a solution of 0.15 g (0.303 mmol) of $[Cu(hfac)_2]\cdot H_2O$ (hfac = hexafluoroacetylacetonate) dissolved in 15 mL of hot *n*-heptane were added 0.17 g (0.202 mmol) of $[Ln(hfac)_3]\cdot 2H_2O$ and 0.02 g (0.101 mmol) of N_3tempo under stirring. The resulting solution was cooled to 10 °C, and after a few days, dark green single crystals were obtained. $C_{49}H_{29}Cu_3F_{48}N_4O_{21}Gd_2$ **1**: Yield = 14.3%; IR (KBr disk, ν_{max}/cm^{-1}): 2121 s (NN), 1649 vs (CO), 1351 w (NO), 1255 vs (CF), 1142 vs, 1102 s. $C_{49}H_{29}Cu_3F_{48}N_4O_{21}Tb_2$ **2**: Yield = 17.3%; IR (KBr disk, ν_{max}/cm^{-1}): 2123 s (NN), 1647 vs (CO); 1351 w (NO), 1252 vs (CF), 1139 vs, 1101 s. $C_{49}H_{29}Cu_3F_{48}N_4O_{21}Dy_2$ **3**: Yield = 18.4%; IR (KBr disk, ν_{max}/cm^{-1}): 2106 s (NN), 1645 vs (CO), 1352w (NO), 1251 vs (CF), 1134 vs, 1100 s.

$[CuLn_2(hfac)_8(H_2O)_2(N_3tempo)_2]$. Ln = Gd^{III} (**4**), Dy^{III} (**5**): To a solution of 0.036 g (0.076 mmol) of $[Cu(hfac)_2]\cdot H_2O$ dissolved in 15 mL of hot *n*-heptane were added 0.123 g (0.152 mmol) of $[Ln(hfac)_3]\cdot 2H_2O$ and 0.03 g (0.152 mmol) of N_3tempo under stirring. The resulting solution was cooled to 10 °C, and after a few days, green single crystals were obtained. $C_{58}H_{42}CuF_{48}N_8O_{20}Gd_2$ **4:** Yield = 24.0%; IR (KBr disk, ν_{max}/cm^{-1}): 2106 s (NN), 1645 vs (CO), 1351 w(NO), 1251 vs (CF), 1134 vs, 1100 s. $C_{58}H_{42}CuF_{48}N_8O_{20}Dy_2$ **5**: Yield = 28.0%; IR (KBr disk, ν_{max}/cm^{-1}): 2098 s (NN), 1648 vs (CO), 1357 w (NO), (CF) 1250 vs, 1134 vs, 1100 s.

X-ray Diffraction. Single-crystal X-ray diffraction data for compounds **1**, **3**, **4**, and **5** were collected on a Oxford GEMINI A Ultra diffractometer with Mo Kα (λ = 0.710 73 Å) radiation at low temperature (120 K), while for **2**, these data were collected using a STOE IPDS II diffractometer operating with Mo Kα (λ = 0.710 73 Å) X-ray tube with graphite monochromator. Data collection, reduction, and cell refinement were performed by Crysalis Red, Oxford Diffraction Ltd. program Version 1.171.32.38[28] for **1**, **3**, **4**, and **5**. The five crystal structures were solved and refined using ShelXS-97 and ShelXL-97 packages.[29] An empirical isotropic extinction parameter *x* was refined, according to the method described by Larson;[30] a multiscan absorption correction was applied.[31] Single crystals of compounds **1** and **3** presented disorder in the N_3tempo azide group, which was modeled with two possible arrangements. The structures were drawn by ORTEP-3 for Windows[32] and Mercury programs.[33] Summary of the crystal structure, data collection, and refinement for compounds **1**−**5** are listed in Supporting Information (SI), in Tables S1 and S2. Selected bond lengths and angles are summarized in Tables 1−3. SI, Figures S1 and S2 show the ORTEP representations of the asymmetric units for compounds **1**−**5**.

Magnetic Measurements. Direct current (dc) magnetic measurements were performed on a Cryogenic Sx600 SQUID magnetometer in the temperature range of 2−280 K. The sample was placed in a gelatin capsule, and the magnetic data were corrected for the contribution of the sample holder. The sample diamagnetism correction was estimated from Pascal's constants. Alternating current (ac) measurements were performed on a Quantum Design PPMS/ACMS system using the same sample.

RESULTS AND DISCUSSION

Two families of heterospin 2p−3d−4f complexes were obtained by reacting a mixture of bis(hexafluoroacetylacetonate) complexes, namely, $[Cu(hfac)_2]\cdot H_2O$ and $[Ln(hfac)_3]\cdot 2H_2O$, with 4-azido-2,2,6,6-tetramethylpiperidine-1-oxyl (N_3tempo). Three pentanuclear $[Cu_3Ln_2(hfac)_8(OH)_4(N_3tempo)]$ (Ln = Gd **1**, Tb **2**, Dy **3**) and two trinuclear $[CuLn_2(hfac)_8(H_2O)_2(N_3tempo)_2]$ (Ln = Gd **4** and Dy **5**) neutral species are formed. A tempo derivative functionalized with a coordinating group was chosen to facilitate the aggregation of the three spin carriers within the same molecular entity. The use of different molar ratios of the reagents allows a good control over the nature of the final products. The excess of copper(II) ions (the pentametallic family) seems to favor the deprotonation of the water molecules, resulting in hydroxo ions that act as bridging ligands.

Description of the Structures. *$[Cu_3Ln_2(hfac)_8(OH)_4(N_3tempo)]$.* Complexes (**1**−**3**). The five metal ions are held together by four hydroxo bridges, as well as by oxygen atoms arising from eight $hfac^-$ ligands. The three

dx.doi.org/10.1021/ic5008044 | Inorg. Chem. 2014, 53, 7508−7517

Table 1. Selected Bond Lengths, Distances (Å) for Compounds 1, 2, and 3

	1	2	3
distances	Ln = Gd^{III}	Ln = Tb^{III}	Ln = Dy^{III}
Cu1—O2	2.553(7)	2.523(8)	2.487(5)
Cu1—O7	1.933(6)	1.937(7)	1.928(5)
Cu1—O10	1.946(6)	1.941(8)	1.938(4)
Cu1—O17	1.937(6)	1.926(9)	1.936(5)
Cu1—O18	1.917(6)	1.920(1)	1.913(6)
Cu2—O8	1.907(6)	1.899(8)	1.912(5)
Cu2—O19	1.871(6)	1.906(9)	1.887(6)
Cu2—O20	1.963(6)	1.977(9)	1.958(6)
Cu2—O21	1.932(6)	1.954(9)	1.936(5)
Cu2—O5	2.646(6)		2.645(5)
Cu3—O2	2.498(6)	2.759(9)	2.469(4)
Cu3—O9	1.915(6)	1.917(7)	1.909(5)
Cu3—O10	1.936(6)	1.954(8)	1.925(5)
Cu3—O15	1.919(7)	1.900(1)	1.909(5)
Cu3—O16	1.920(6)	1.912(9)	1.920(6)
Ln1—O1	2.353(7)	2.367(9)	2.326(5)
Ln1—O2	2.696(6)	2.524(7)	2.781(6)
Ln1—O3	2.406(6)	2.357(8)	2.370(5)
Ln1—O4	2.334(6)	2.410(1)	2.317(5)
Ln1—O5	2.426(6)	2.347(9)	2.402(5)
Ln1—O6	2.398(7)	2.415(8)	2.366(5)
Ln1—O7	2.436(5)	2.458(7)	2.416(5)
Ln1—O8	2.489(5)	2.512(8)	2.442(5)
Ln1—O9	2.429(6)	2.424(8)	2.388(4)
Ln2—O7	2.417(5)	2.400(8)	2.380(5)
Ln2—O8	2.387(5)	2.370(7)	2.365(5)
Ln2—O9	2.414(6)	2.388(8)	2.398(5)
Ln2—O10	2.448(6)	2.419(7)	2.423(5)
Ln2—O11	2.377(7)	2.350(1)	2.357(5)
Ln2—O12	2.317(6)	2.340(1)	2.298(6)
Ln2—O13	2.367(6)	2.352(9)	2.335(5)
Ln2—O14	2.354(6)	2.352(8)	2.340(4)
Cu1···Cu3	3.232(2)	3.201(2)	3.212(1)
Cu1···Ln1	3.805(1)	3.766(1)	3.795(1)
Cu1···Ln2	3.393(1)	3.426(2)	3.372(1)
Cu2···Ln1	3.768(1)	3.905(2)	3.741(1)
Cu2···Ln2	3.755(1)	3.720(1)	3.742(1)
Cu3···Ln1	3.731(1)	3.802(1)	3.721(1)
Cu3···Ln2	3.422(1)	3.386(2)	3.397(1)
Ln1···Ln2	3.6348(5)	3.6230(7)	3.5817(5)

Table 2. Selected Bond Angles (deg) for Compounds 1, 2, and 3

	1	2	3
angles	Ln = Gd^{III}	Ln = Tb^{III}	Ln = Dy^{III}
Cu1—O2—Cu3	79.6(2)	74.4(2)	80.8(2)
Cu1—O10—Cu3	112.7(3)	110.5(4)	112.5(2)
Cu1—O2—Ln1	92.9(2)	96.5(3)	92.0(2)
Cu1—O7—Ln1	120.7(3)	117.4(3)	121.4(2)
Cu1—O7—Ln2	102.0(2)	103.9(3)	102.5(2)
Cu1—O10—Ln2	100.5(2)	103.0(3)	100.7(2)
Cu2—O5—Ln1	95.9(2)		95.5(2)
Cu2—O8—Ln1	117.4(3)	120.9(4)	118.0(2)
Cu3—O2—Ln1	91.8(2)	91.9(3)	90.1(2)
Cu3—O9—Ln1	117.9(3)	121.9(4)	119.6(2)
Cu3—O9—Ln2	103.9(2)	103.2(3)	103.5(2)
Gd1—O7—Ln2	97.0(2)	96.4(3)	96.6(2)
Gd1—O9—Ln2	97.3(2)	97.7(3)	96.9(2)
O2—Cu1—O7	78.5(2)	77.1(3)	80.0(2)
O2—Cu1—O17	100.0(2)	112.0(4)	100.5(2)
O7—Cu1—O18	171.1(3)	96.0(4)	170.7(2)
O7—Cu1—O10	85.0(3)	83.9(3)	84.2(2)
O10—Cu1—O17	174.3(4)	87.9(4)	173.8(2)
O17—Cu1—O18	93.3(3)	92.1(4)	93.0(2)
O2—Cu3—O9	81.3(2)	74.3(3)	82.2(2)
O2—Cu3—O16	104.9(2)	110.0(3)	103.1(2)
O9—Cu3—O10	84.7(2)	83.8(3)	84.5(2)
O9—Cu3—O15	91.5(3)	90.8(4)	92.0(2)
O10—Cu3—O16	90.9(3)	92.2(4)	91.1(4)
O15—Cu3—O16	92.9(3)	93.3(4)	92.4(2)
O8—Cu2—O20	92.6(3)	91.2(3)	92.2(2)
O8—Cu2—O21	92.6(3)	85.4(4)	84.2(2)
O19—Cu2—O20	92.0(3)	91.7(4)	92.4(2)
O19—Cu2—O21	91.6(3)	91.7(4)	91.2(2)
N1—O21—Cu2	123.2(5)	122.3(9)	123.6(4)

compounds have similar structures; compounds **1** and **3** are isomorphous (monoclinic, $P2_1/n$), while compound **2** crystallizes in the $P2_1/c$ monoclinic space group. The molecular structures for compounds **1**−**3** are presented in Figure 1. Apart from the slight differences between them (see below), the pentanuclear cores in the three compounds are constructed in a similar way.

First of all, it is important to highlight that two out of the eight $hfac^-$ molecules (labeled **A** and **B** in Figure 1) act as bridging ligands, while the six others (**C**−**H**) are coordinated solely to one metal center (either Cu^{II} or Ln^{III}). The metal ions in the core are bridged by four hydroxo (O7, O8, O9, and O10) and by the **A** and **B** $hfac^-$ ligands. The molecule **A** is coordinated through O1 to Ln1, whereas the O2 atom bridges three metal ions (Cu1, Cu2, and Ln1). The molecule **B** is coordinated through O6 to Ln1 and through O5 simultaneously to Ln1 and Cu2 only in the Gd^{III} and Dy^{III} derivatives. The N_3tempo organic radical is coordinated through its oxygen atom to the basal plane of the Cu2 ion. The three copper ions are pentacoordinated with slightly distorted square-pyramidal geometries in **1** and **3**. Cu1 is coordinated in the basal plane by the **D** $hfac^-$ ligand and by two hydroxo-bridging groups (O7 and O10), which connect Cu1 to Ln1 and Ln2 (O7) and to Cu3 and Ln2 (O10). The apical position is occupied by an oxygen atom, O2, arising from the **A** ligand [Cu1−O2 = 2.553(7) in **1**, 2.523(8) in **2**, and 2.485(5) Å in **3**]. This oxygen atom connects three metal ions: Cu1, Cu3, and Ln1. The Cu1−O distances in the basal plane vary between 1.916(6) and 1.946(6) for **1**, between 1.920(1) and 1.941(8) for **2**, and between 1.911(6) and 1.936(4) Å for **3**. The trigonal distortion from the square pyramidal geometry is evaluated by the τ parameter, defined as $\tau = [(\theta - \phi)/60]$,[34] where θ and ϕ are the largest and second-largest angles between the donor atoms forming the basal plane in square-pyramidal geometry ($\theta > \phi$). The value of the τ parameter for Cu1 is 0.04 in **1**, 0.07 in **2**, and 0.03 in **3**. The Cu2 ion is coordinated in the basal plane by one $hfac^-$ chelating ligand (**H**), one nitroxide oxygen atom (O21), and one oxygen atom (O8) from the hydroxo ligand, which links Cu2 to Ln1 and Ln2. In compounds **1** and **3**, the apical position of Cu2 is occupied by an oxygen atom (O5) arising from the **B** ligand connecting Cu2 to Ln1 (Cu2−O5 = 2.646(6) in **1** and 2.645(5) Å in **3**). The value of the τ parameter for the Cu2 is 0.01 in **1** and 0.003 in **3**. The remarkable difference between the terbium derivative, **2**, when

dx.doi.org/10.1021/ic5008044 | Inorg. Chem. 2014, 53, 7508−7517

Table 3. Selected Bond Lengths, Distances (Å), and Angles (deg) for Compounds 4 and 5

	4	5		4	5
bonds	Ln = Gd^{III}	Ln = Dy^{III}	angles	Ln = Gd^{III}	Ln = Dy^{III}
Cu1—O9	1.936(5)	1.933(5)	O9—Cu1—O10	92.7(2)	92.8(2)
Cu1—O10	1.940(7)	1.937(5)	O11—Cu1—O12	92.9(2)	92.6(2)
Cu1—O11	1.917(5)	1.915(5)	O9—Cu1—O12	89.4(2)	89.5(2)
Cu1—O12	1.944(6)	1.943(5)	O10—Cu1—O11	84.8(2)	85.0(2)
Cu1—N2	2.656(6)	2.663(6)	O9—Cu1—N2	87.3(2)	87.2(2)
Cu1—N5	2.477(6)	2.476(6)	O9—Cu1—N5	87.9(2)	88.1(2)
Ln1—O1	2.410(5)	2.365(5)	O1—Ln1—O2	70.4(2)	71.1(1)
Ln1—O2	2.408(5)	2.392(5)	O3—Ln1—O4	71.1(2)	71.5(1)
Ln1—O3	2.372(5)	2.349(5)	O5—Ln1—O6	72.3(2)	72.5(2)
Ln1—O4	2.321(5)	2.304(5)	O7—Ln1—O8	70.6(2)	70.6(2)
Ln1—O5	2.326(4)	2.441(5)	Ln1—O7—N1	160.0(4)	159.9(4)
Ln1—O6	2.457(5)	2.289(4)	O14—Ln2—O15	70.9(2)	71.7(2)
Ln1—O7	2.353(4)	2.333(4)	O16—Ln2—O17	74.2(2)	75.3(2)
Ln1—O8	2.388(5)	2.364(5)	O18—Ln2—O19	71.5(2)	71.9(2)
Ln2—O13	2.288(5)	2.270(5)	O13—Ln2—O20	95.0(2)	95.0(2)
Ln2—O14	2.353(6)	2.337(5)	Ln2—O13—N8	148.4(4)	145.7(4)
Ln2—O15	2.431(4)	2.407(4)			
Ln2—O16	2.341(6)	2.308(5)			
Ln2—O17	2.409(5)	2.376(4)			
Ln2—O18	2.404(4)	2.375(4)			
Ln2—O19	2.386(5)	2.358(5)			
Ln2—O20	2.386(5)	2.373(5)			
Ln1···Cu1	9.645(1)	9.512(1)			
Ln2···Cu1	9.547(1)	9.6307(9)			

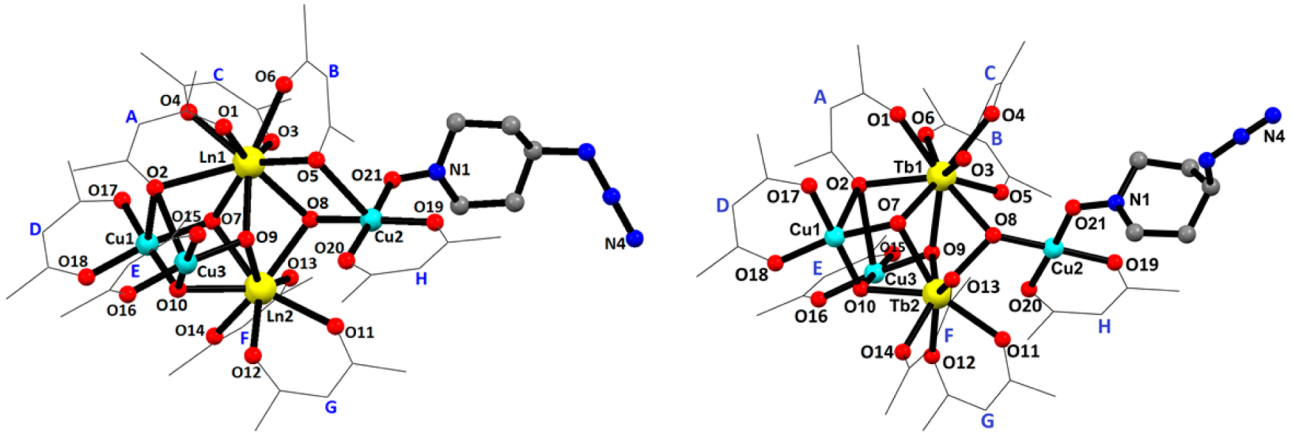

Figure 1. Crystal structures of the pentametallic compounds **1** and **3** (left) and **2** (right). The disorder in the azide group (**1** and **3**), the N_3tempo methyl groups, and the hydrogen and fluorine atoms were omitted for sake of clarity.

compared with compounds **1** and **3** consists in the coordination environment of Cu2, which is tetracoordinated, with a slightly distorted square-planar geometry (see Figure 1, right). The Cu2−O distances within the basal plane vary between 1.871(6) and 1.963(6) in **1**, between 1.899(8) and 1.906(8) in **2**, and between 1.891(6) and 1.958(5) Å in **3**. The Cu−O21 bond length (O21 arises from the N_3tempo ligand) is slightly shorter in **1** when compared with **2** and **3**: Cu2−O21 = 1.932(6), 1.954(9), and 1.936(5) Å, respectively. The coordination environment of Cu3 ion is very similar to that of Cu1, the basal plane being occupied by the **E** $hfac^-$ ligand and by two hydroxo-bridging groups (O9 and O10), which further link Cu3 to Ln1 and Ln2 (O9) and Cu3 to Cu1 and Ln2 (O10). The axial position of the Cu3 is occupied by one β-diketonato oxygen atom, O2, from the **A** ligand (Cu3−O2 = 2.498(6) in **1**, 2.759(9) in **2**, and 2.469(4) Å in **3**). The Cu3−O bond lengths within the basal plane vary as follows: 1.915(6)−1.936(6) in **1**, 1.900(1)−1.954(8) in **2**, and 1.909(5)−1.925(5) Å in **3**. The value of the τ parameter for Cu3 is 0.008 in **1**, 0.02 in **2**, and 0.008 in **3**.

The lanthanide ions in the three compounds show similar coordination environments. Ln1 has a coordination number of nine, being coordinated by one terminal $hfac^-$ ligand, **C**, two bridging (**A** and **B**) $hfac^-$ ligands, and by three μ_3-hydroxo bridges (O7, O8, and O9), which link Ln1 to two Cu^{II} ions (Cu1 and Cu3) and to Ln2. The coordination geometry of Ln1 is distorted tricapped trigonal prismatic (Figure 2). The Ln1−$O_{diketonate}$ bond lengths fall in the range of 2.334(6)−2.696(6) in **1**, 2.347(9)−2.524(7) in **2**, and 2.317(5)−2.781(6) Å in **3**, while the Ln1−$O_{hydroxo}$ bond lengths vary between 2.429(6) and 2.489(5) in **1**, between 2.424(8) and 2.512(8) in **2**, and between 2.388(4) and 2.442(5) Å in **3**. The Ln2 ion shows a

dx.doi.org/10.1021/ic5008044 | Inorg. Chem. 2014, 53, 7508−7517

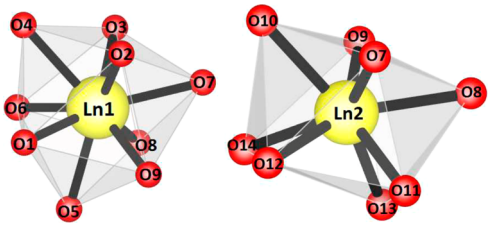

Figure 2. Coordination environments of the lanthanide ions in compounds **1**−**3**.

coordination number of eight with a distorted bicapped trigonal prismatic geometry (Figure 2), being coordinated by two terminal hfac$^-$ ligands (**F** and **G**) and by four μ_3-hydroxo bridges (O7, O8, O9, and O10), which connect Ln2 to the other four metal ions (Cu1, Cu2, Cu3, and Ln1).

The Ln2−$O_{diketonate}$ bond lengths are in the following ranges: 2.317(6)−2.377(7) in **1**, 2.336−2.352(9) in **2**, and 2.298(6)−2.357(6) Å in **3**, while the Ln2−$O_{hydroxo}$ distances are in the range of 2.387(5)−2.448(6) in **1**, 2.370(7)−2.419(7) in **2**, and 2.365(5)−2.423(5) Å in **3**. The metal−metal distances within the pentanuclear complexes are Cu1···Cu3 = 3.232(2); Cu1···Ln1 = 3.805(1); Cu1···Ln2 = 3.393(1); Cu2···Ln1 = 3.768(1); Cu2···Ln2 = 3.755(1); Cu3···Ln1 = 3.731(1); Cu3···Ln2 = 3.422(1); Ln1···Ln2 = 3.6348(5) Å in **1**; Cu1···Cu3 = 3.201(2); Cu1···Ln1 = 3.766(1); Cu1···Ln2 = 3.426(2); Cu2···Ln1 = 3.905(2); Cu2···Ln2 = 3.720(1); Cu3···Ln1 = 3.802(1); Cu3···Ln2 = 3.386(2); Ln1···Ln2 = 3.6230(7)Å in **2**; Cu1···Cu3 = 3.212(1); Cu1···Ln1 = 3.795(1); Cu1···Ln2 = 3.372(1); Cu2···Ln1 = 3.741(1); Cu2···Ln2 = 3.742(1); Cu3···Ln1 = 3.721(1); Cu3···Ln2 = 3.397(1); Ln1···Ln2 = 3.5817(5) Å in **3**. Selected bond distances and angles for compounds **1**−**3** are gathered in Tables 1 and 2.

The analysis of the packing diagrams for crystals **1**−**3** (Figure 3) reveals the formation of supramolecular chains supported by hydrogen bonds established between one hydroxo group from one molecule and an azide nitrogen atom from another one (O10···N4B^{i} = 2.823(14) Å for **1**; O10···N4^{ii} = 2.89(2) Å for **2**; N4B···O10^{iii} = 2.833(12) Å, for **3**; i = $-x + 1/2, y + 1/2, -z + 1/2$, ii = $x, -y - 1/2, z - 1/2$; iii = $-x + 1/2, y + 1/2, -z + 1/2$).

[CuLn$_2$(hfac)$_8$(H$_2$O)$_2$(N$_3$tempo)$_2$]. Complexes **4** and **5**. The crystal structures of the isostructural compounds **4** and **5** (Figure 4) consist of U-shaped neutral trimetallic species containing one Cu^{II} and two Ln^{III} ions (Gd^{III} **4** and Dy^{III} **5**).

The structure can be described as resulting from two {Ln(hfac)$_3$(N$_3$tempo)} units that act, through their nitrogen atoms (N2 and, respectively, N5) from the N_3 groups, as metalloligands toward the copper ion from a {Cu(hfac)$_2$} unit.

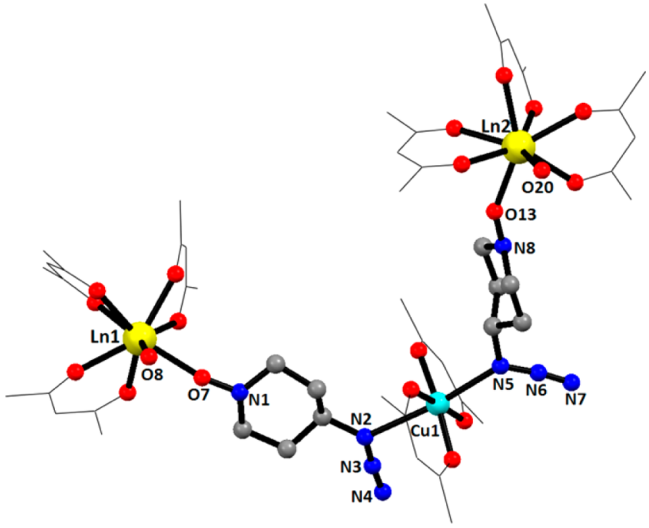

Figure 4. Crystal structure of compounds **4** and **5**. N_3tempo methyl groups, and hydrogen and fluorine atoms were omitted for sake of clarity.

The two nitrogen atoms are coordinated into the apical positions of the copper(II) ion, which is therefore hexacoordinated, with an elongated octahedral geometry. The Cu−N_{azide} (Cu1−N2 and Cu1−N5) bond distances are 2.653(6) and 2.477(6) Å in **4** and 2.662(6) and 2.476(6) Å in **5**. These bond distances are similar to the previously reported ones for the [Cu(hfac)$_2$(N$_3$tempo)]$_n$ chain.[15c] Each {Ln(hfac)$_3$(N$_3$tempo)} moiety results from the coordination of the organic radical, through the nitroxide oxygen atom, to the lanthanide ion. The two crystallographically nonequivalent lanthanide ions are coordinated by three hfac$^-$ chelating ligands, one nitroxide oxygen atom (Gd1−O7 = 2.353(4), Gd2−O13 = 2.288(5) Å; Dy1−O7 = 2.333(4), Dy2−O13 = 2.270(5) Å), and one aqua ligand (Gd1−O8 = 2.388(5), Gd2−O20 = 2.390(5) Å; Dy1−O8 = 2.364(5), Dy2−O20 = 2.373(5)Å). The coordination geometry of lanthanide ions Ln1 and Ln2 in these compounds is distorted bicapped trigonal prismatic. The Ln−$O_{diketonate}$ distances vary between 2.321(5) and 2.457(5) Å (in **4**) and between 2.289(4) and 2.441(5) Å (in **5**). The intramolecular Cu···Ln distances are slightly larger for the gadolinium derivative [Gd1···Cu1 = 9.645(1) and Gd2···Cu1 = 9.547(1) Å] when compared with the dysprosium derivative [Dy1···Cu1 = 9.6307(9) Å and Dy2···Cu1 = 9.512(1) Å]. Selected bond distances and angles for compounds **4** and **5** are gathered in Table 3.

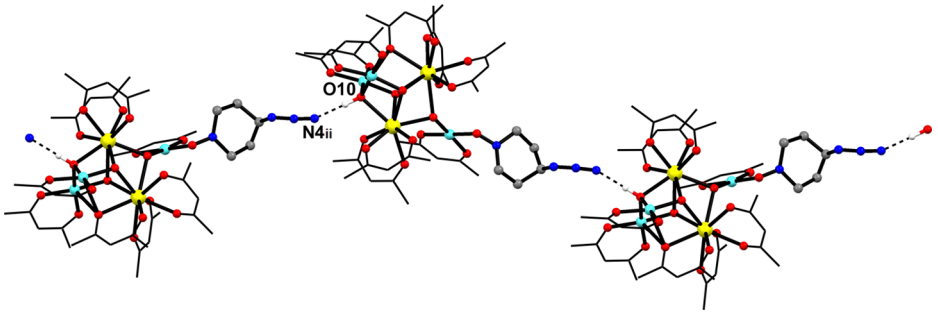

Figure 3. Hydrogen bonds in compound **2**. Symmetry code: ii = $x, -y - 1/2, z - 1/2$.

dx.doi.org/10.1021/ic5008044 | Inorg. Chem. 2014, 53, 7508−7517

Intermolecular hydrogen bonding between an hfac$^-$ oxygen atom (O5) and the aqua ligand from another molecule leads to supramolecular dimers, as shown in Figure 5 (O5···O20*i* = 2.865(5) and O8i···O15 = 2.850(6) Å, symmetry operation i: $-x$, $2 - y$, $1 - z$).

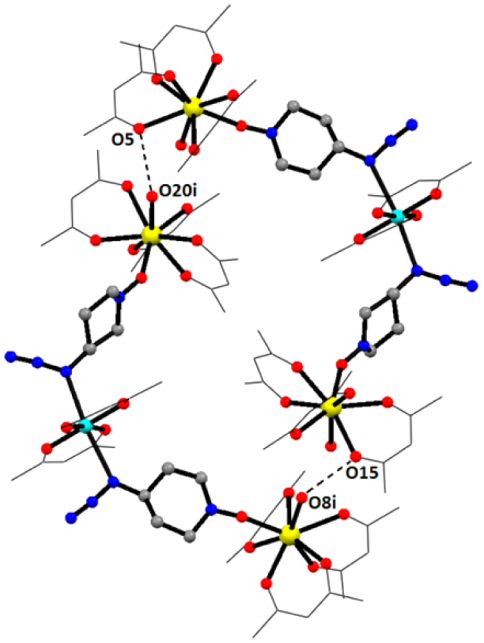

Figure 5. Formation of supramolecular dimers through H-bond interactions in compounds **4** and **5**. Symmetry code: i = $-x$, $2 - y$, $1 - z$. N_3tempo methyl groups, and hydrogen and fluorine atoms were omitted for sake of clarity.

Magnetic Properties of the Gadolinium Derivatives 1 and 4. The magnetic properties of compound **1** were investigated in the temperature range of 2−280 K, and the plot of $\chi_M T$ versus T, where χ_M is the molar magnetic susceptibility, is shown in Figure 6. At 280 K, the value of $\chi_M T$, 16.8 cm^3 mol^{-1} K, is lower than the expected one for uncoupled three Cu^{II} ions, two Gd^{III} ions plus one radical (17.3 cm^3 mol^{-1} K). On lowering temperature, $\chi_M T$ slightly decreases down to 16.5 cm^3 mol^{-1} K around 220 K then remains constant and decreases furthermore at lower temperatures. Since Gd^{III} has a $^8S_{7/2}$ ground term, with no orbital contribution, the decrease of $\chi_M T$ comes from predominant antiferromagnetic interactions among the spin carriers within the compound. On the basis of the crystal structure of compound **1**, up to nine magnetic exchange interactions should be taken into account, namely Cu2−Rad, Cu2−Gd1, Cu2−Gd2, Cu1−Cu3, Cu1−Gd1, Cu1−Gd2, Cu3−Gd1, Cu3−Gd2 and Gd1−Gd2 (Figure 1). However, the value of the Cu1−O10−Cu3 angle [112.7(3)°] involving basal positions of the two copper ions is much larger than 97.5° and a very strong antiferromagnetic interaction occurs between Cu1 and Cu3.[35] The high temperature decrease of $\chi_M T$ on lowering temperature results from this interaction. Indeed, the value of 16.5 cm^3 mol^{-1} K corresponds to the theoretical one for two uncoupled Gd^{III} ions plus two $S = 1/2$ spins. Therefore, below 220 K, the magnetic behavior of compound **1** can be investigated on the basis of four interacting spins, namely, two $S = 1/2$ and two $S = 7/2$.

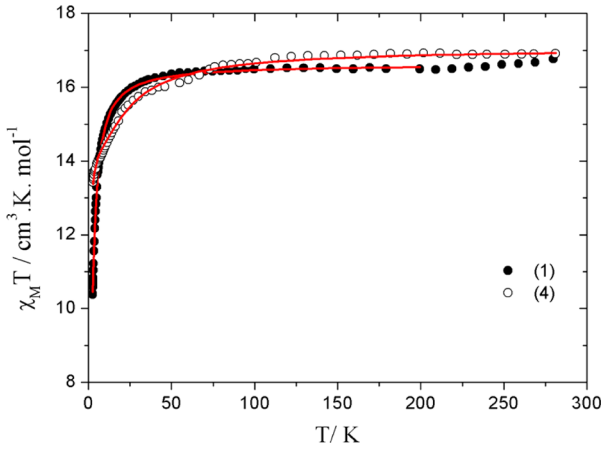

Figure 6. Thermal dependence of the $\chi_M T$ product for **1** (●) and **4** (○) at H = 1 kOe. Solid lines represent the best fit.

To avoid any overparametrization, the attempt to reproduce the magnetic data considered only the interactions between Cu2 and the N_3tempo radical, and between Gd1 and Gd2, within an isotropic spin Hamiltonian (eq 1).

$$\hat{H} = -J_1(\vec{S}_{Cu2}\cdot\vec{S}_{Rad}) - J_2(\vec{S}_{Gd1}\cdot\vec{S}_{Gd2}) + \text{Zeeman terms} \quad (1)$$

These calculations were performed with the MagProp routine, available under the program DAVE.[36] The solid line in Figure 6 shows the best fit for compound **1** found with g = 2.01, J_1 = −6.3 cm^{-1}, and J_2 = −0.13 cm^{-1}. Concerning the Cu^{II}(square pyramid)−Rad$^\bullet$ coupling, its nature depends on the coordination position of the nitroxide radical: if this one is located in the apical position, the two magnetic orbitals (π^* and $d_{x^2-y^2}$) are orthogonal, and the interaction is expected to be ferromagnetic, while the basal location of the nitroxide radical favors an antiferromagnetic interaction.[37] Since in compound **1** the N_3tempo ligand is coordinated in the basal plane of the copper ion, this exchange interaction is expected to be antiferromagnetic. The obtained Gd^{III}−Gd^{III} coupling constant is within the range observed for other compounds previously reported.[38] It is noteworthy that this simple model reproduces also very well the isothermal field dependence of the magnetization at 1.8 K, shown in Figure 7.

The plot of $\chi_M T$ versus T for compound **4** is also shown in Figure 6. The high-temperature value of 16.9 cm^3 mol^{-1} K corresponds to the expected value for one Cu^{II} ion, two Gd^{III} ions, and two radicals. When the compound is cooled, the $\chi_M T$ value remains mainly constant and decreases at lower temperatures. Given that Gd^{III} does not present anisotropy the decrease of the $\chi_M T$ value comes from predominant antiferromagnetic interactions among the spin carriers. In compound **4**, the copper(II) ion is coordinated to the zero spin density azide nitrogen atoms; thus, only the magnetic interactions between gadolinium and radicals were considered. A careful analysis of the crystal structure revealed that the coordination geometry of the radical to both gadolinium(III) site presents quite different Gd−O−N angles and Gd−O distances. Therefore, the magnetic data were reproduced by an isotropic spin Hamiltonian (eq 2), which considers two different exchange interactions and an isolated copper ion:

$$\hat{H} = -J_1(\vec{S}_{Gd1}\cdot\vec{S}_{Rad1}) - J_2(\vec{S}_{Gd2}\cdot\vec{S}_{Rad2}) + \text{Zeeman terms} \quad (2)$$

dx.doi.org/10.1021/ic5008044 | Inorg. Chem. 2014, 53, 7508−7517

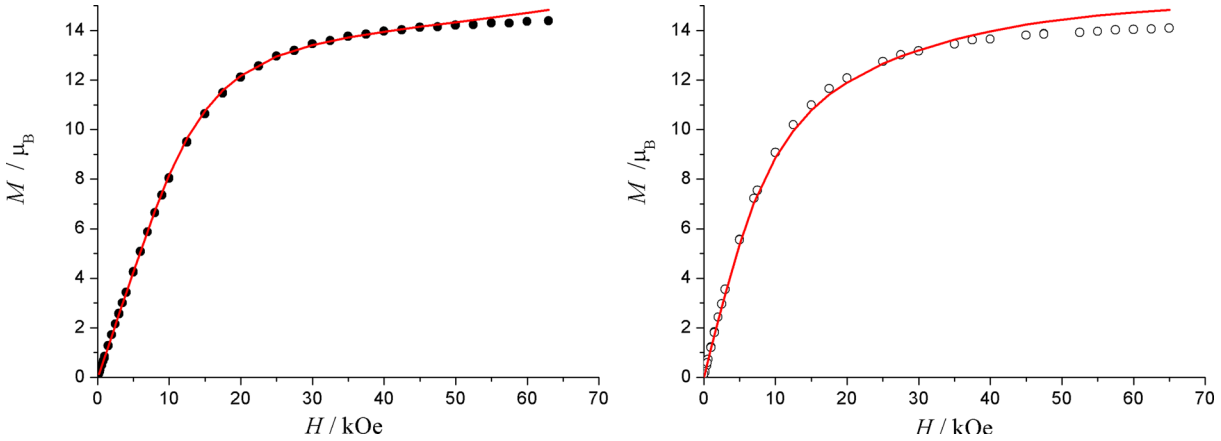

Figure 7. M vs H plots for **1** (left) at 1.8 K and **4** at 2 K (right). The solid lines represent the simulations for **1** and **4** (vide text).

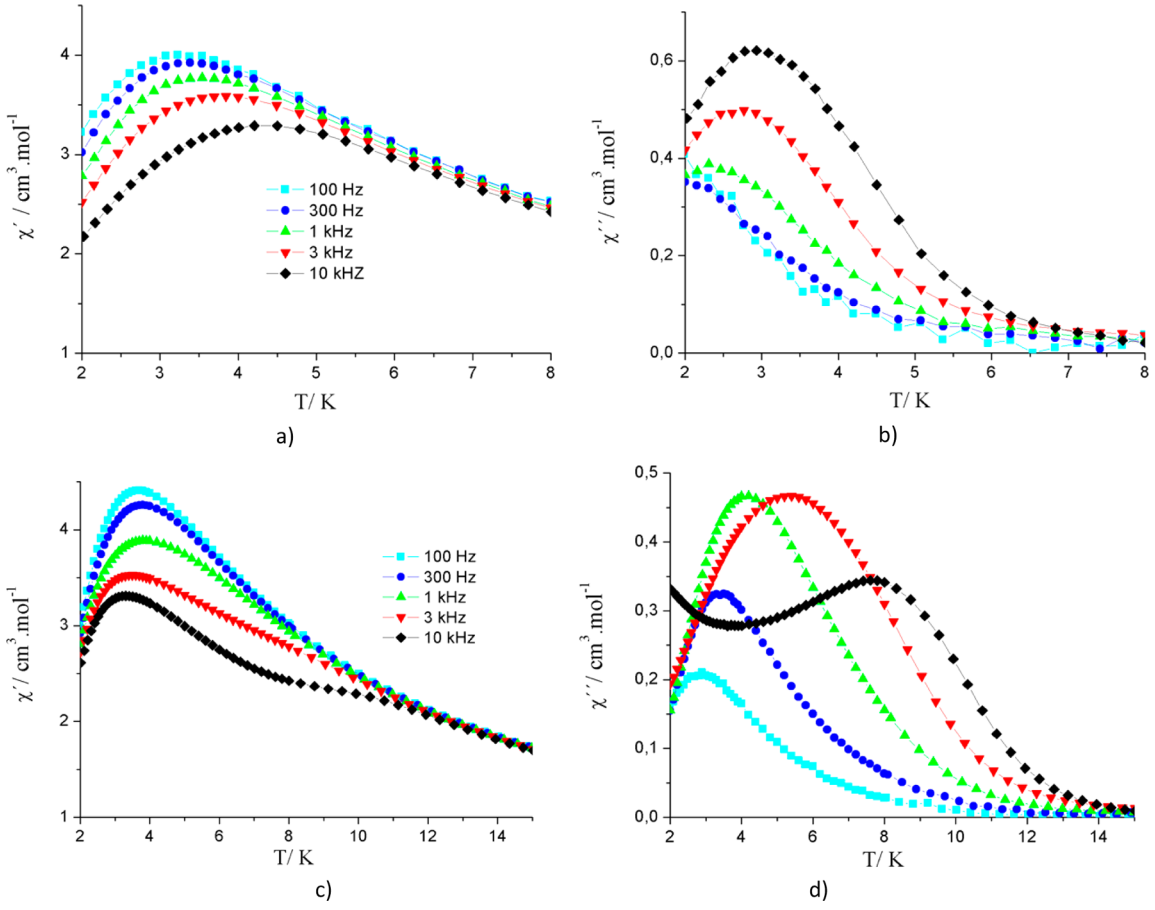

Figure 8. Susceptibility data (ac) between 100 Hz and 10 kHz from 2 to 15 K for compounds **3** (a and b) and **5** (c and d): in-phase, χ' (a and c) and out-phase, χ'' (b and d) ac signals.

The magnetic fit was also carried out using the Magprop routine.[36] The solid line in Figure 6 shows the best fit for compound **4** found with $g = 2.02$, $J_1 = -6.9$ cm^{-1}, and $J_2 = -0.7$ cm^{-1}. The obtained Gd^{III}–$Rad^{\bullet}$ coupling constants are within the range observed for other compounds previously reported.[39,40] The antiferromagnetic nature of the Gd^{III}–$Rad^{\bullet}$ interactions is also confirmed by the isothermal magnetization versus magnetic field measurements (Figure 7). At 2 K, the ground state corresponds to two $S = 3$ and one $S = 1/2$ uncorrelated spins. As J_2 is small, magnetic fields higher than 20 kOe might overcome this antiferromagnetic interaction, and therefore the magnetization value at 65 kOe (14.1 μ_B) is higher than the expected one for two $S = 3$ and one $S = 1/2$ spins (13 μ_B) but lower than the one for two $S = 7/2$ and three $S = 1/2$ spins (17 μ_B). Furthermore, the isothermal magnetization M versus H/T curves at 2 and 4 K (Figure S3 in the SI) corroborate this ground state with a very good superposition at low fields and a slight deviation at high fields coming from the weak J_2 interaction as explained before.

Magnetic Properties of Compounds 2, 3 and 5. The plots of $\chi_M T$ versus T for compounds **2**, **3**, and **5** are shown in Figure S4 in the SI. The room-temperature values are 23.6 (for

dx.doi.org/10.1021/ic5008044 | Inorg. Chem. 2014, 53, 7508–7517

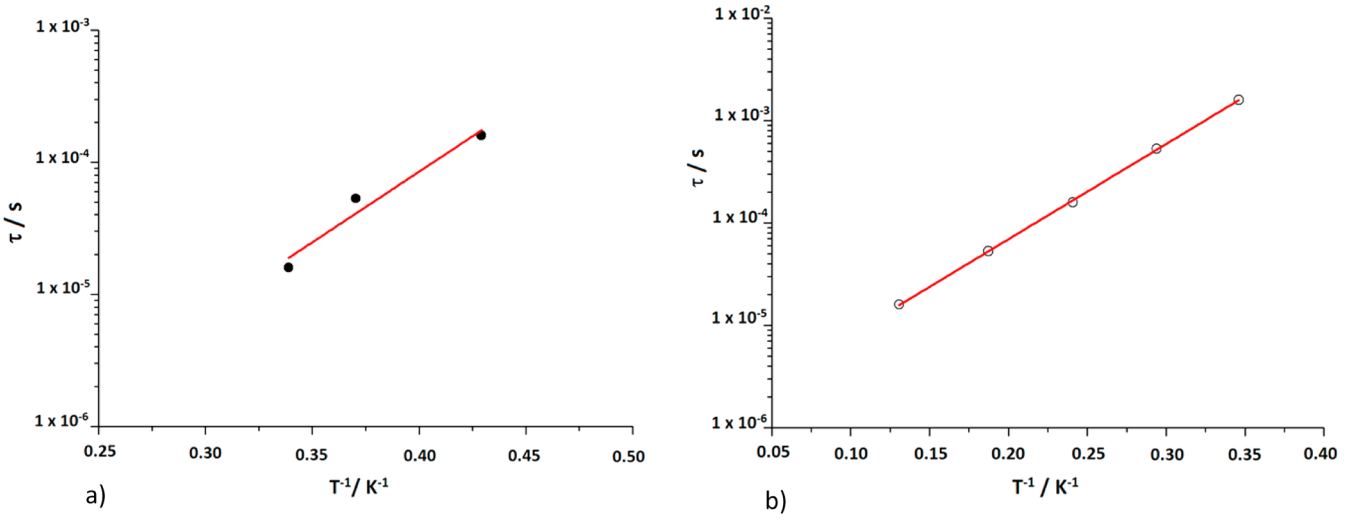

Figure 9. Arrhenius plot from the out-of-phase peak at H = 4 kOe for **3** (a) and **5** (b).

2), 28.5 (for **3**), and 27.8 cm^3 mol^{-1} K (for **5**), slightly lower than the expected spin-only values for noninteracting ions (25.1, 29.8, and 29.5 cm^3 mol^{-1} K, respectively). As explained for compound **1**, a very strong antiferromagnetic interaction occurs between Cu1 and Cu3 also in compounds **2** and **3**, leading to an expected high-temperature value corresponding to two uncoupled Ln^{III} ions plus two $S = 1/2$ spins (24.4 for **2** and 29.1 for **3**). For these three compounds, the decrease of $\chi_M T$ with cooler temperatures can result from the depopulation of excited Stark sublevels, antiferromagnetic interactions, and/or significant magnetic anisotropy.

Dynamic Magnetic Properties. The dynamic magnetic properties of compounds **2**, **3**, and **5** were investigated by temperature- and frequency-dependent ac magnetic susceptibility measurements. No clear frequency dependence was evidenced in any compound under H = 0 Oe static magnetic field. However, it is well-known that in SMM the energy barrier responsible for the relaxation process can be tuned by a magnetic field, suppressing, for instance, the quantum tunneling by removing the quasi-degeneracy of the ground states. Therefore, the ac susceptibilities were also measured under a static magnetic field. With H = 1500 Oe, compound **2** exhibits slow relaxation of its magnetization, with a slight frequency dependence of the in-phase (χ') susceptibility (Figure S5 in the SI), although no maxima in the in-phase (χ') or out-of-phase (χ'') susceptibilities could be observed above 2 K. Under H = 4 kOe, compounds **3** and **5** exhibit frequency-dependent maxima in both in-phase (χ') and out-of-phase (χ'') susceptibilities (Figure 8).

For these compounds, the in-phase and out-of-phase signals moved to higher temperatures with field, which is a signature of the presence of quantum tunneling of the magnetization in zero field. For **3**, the relaxation time obtained from the out-of-phase susceptibility peaks was fitted to an Arrhenius law (Figure 9a), giving an energy barrier of $\Delta E/k_B$ = 24 K and a pre-exponential factor $\tau_0 = 5 \times 10^{-9}$ s, within the range of values for SMMs.[41] Furthermore, the value of the relative variation of χ'' peak temperature (T_f) per decade frequency ($K = \Delta T_f / [T_f \Delta(\log f)]$) is 0.12 for compound **3**, which is close to the typical value for compounds with superparamagnetic behavior (0.28).[42,43] For compound **5**, the shape of the magnetic susceptibilities under H = 4 kOe does not look like that of a classical SMM with a single relaxation process. Indeed, the broad out-of-phase susceptibility peaks reflect the presence of a distribution of relaxation time. The width of this distribution can be directly accessed from the Cole−Cole plots (Figure 10), introducing

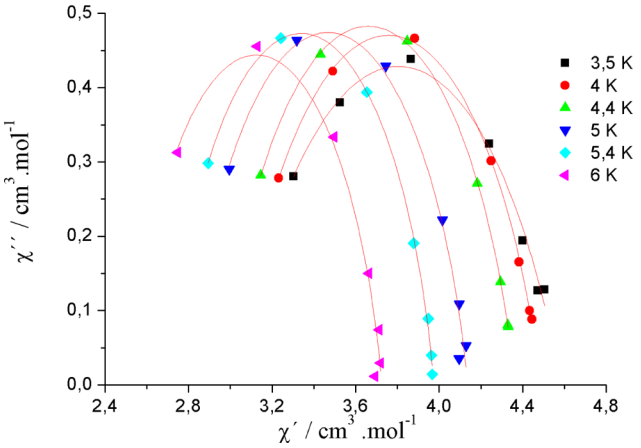

Figure 10. Cole−Cole plots for compound **5**.

the α parameter in the Debye formula.[44] On lowering temperature, the distribution broadens and α changes from 0.18 at 6 K to 0.37 at 3.5 K. The Arrhenius plot from the out-of-phase susceptibility peaks is shown in Figure 9b, leading to an energy barrier of $\Delta E/k_B$ = 21 K and a pre-exponential factor $\tau_0 = 1 \times 10^{-6}$ s, larger than typical values for SMMs.[41] This larger pre-exponential factor suggests that the applied field of 4 kOe suppressed only partially the quantum pathway of relaxation. The value of the relative variation of χ'' peak temperature (T_f) per decade frequency is 0.14 for compound **5**, which is close to the value for superparamagnets. Moreover, one must stress the shape of the in-phase susceptibility for the highest frequencies as well as the increase at low temperature of the 10 kHz out-of-phase χ'' susceptibility. Indeed, such behavior may suggest the presence of another relaxation process at lower temperature, which seems coherent with the presence of two distinct Dy ions in the crystal structure of compound **5**. Measurements at much lower temperature would be very helpful to seek better insight into the other possible relaxation processes. Finally, the dynamic properties of compounds **3** and **5** are consistent with an SMM behavior induced by the large

dx.doi.org/10.1021/ic5008044 | Inorg. Chem. 2014, 53, 7508−7517

anisotropy brought by Dy^{III} and the presence of quantum tunneling at zero field.

CONCLUSIONS

We synthesized and characterized two novel families of 2p−3d−4d triheterospin systems. The first family consists of three pentametallic compounds with unprecedented magnetic core (**1**−**3**) in which the metal ions are held together by four hydroxo bridges and eight $hfac^-$ ligands. The second family consists of trimetallic compounds in a U-shaped architecture, as a result of two $\{Ln(hfac)_3(N_3tempo)\}$ units bridged to one $\{Cu(hfac)_2\}$ unit through a radical molecule. Interestingly, it was observed that a small change in stoichiometry of the building blocks used in the reactions favors the water molecules deprotonation leading to the formation of pentametallic compounds. This change allowed us to modulate the final architecture and consequently the magnetic properties of these compounds. The investigation of the dc magnetic properties of compound **1** confirmed the presence of a strong antiferromagnetic interaction involving the copper ions via hydroxo bridges, as well as antiferromagnetic interactions between radical and copper and between gadolinium ions. In the trimetallic compound **4**, it was observed that the antiferromagnetic interactions between Gd^{III} and radicals led to a ground state characterized by uncorrelated two $S = 3$ and one $S = 1/2$ spins at low temperature. The dynamic magnetic properties, under a static magnetic field, revealed that compounds **2**, **3**, and **5** exhibit slow relaxation of the magnetization, with an energy barrier and pre-exponential factor for compounds **3** and **5** consistent with an SMM behavior. The synthetic strategy presented herein is general and can be further developed using a large variety of organic radicals decorated with additional coordinating groups.

ASSOCIATED CONTENT

Supporting Information

The ORTEP representations of the asymmetric units of compounds **1**−**5** are depicted in Figures S1 and S2. The isothermal magnetization M versus H/T curves measured at 2 and 4 K for compound **4** are presented in Figure S3. Figure S4 displays the thermal dependence of the $\chi_M T$ product for compounds **2**, **3**, and **5** at $H = 1$ kOe. The in-phase (χ') ac signal between 30 Hz−10 kHz from 2 to 18 K for compound **2** is depicted in Figure S5. This material is available free of charge via the Internet at http://pubs.acs.org. CCDC No. 992583 to 992587 contain the supplementary crystallographic data for this Paper. These data can be obtained free of charge from The Cambridge Crystallographic Data Centre via www.ccdc.cam.ac.uk/data_request/cif

AUTHOR INFORMATION

Corresponding Authors

*E-mail: mariavaz@vm.uff.br. (M.G.F.V.)
*E-mail: marius.andruh@dnt.ro. (M.A.)

Notes

The authors declare no competing financial interest.

ACKNOWLEDGMENTS

The authors are thankful for financial support provided by FAPERJ and CNPq. We also acknowledge LabCri (Universidade Federal de Minas Gerais, Brazil) for the use of crystallographic facilities. M.A. thanks FAPERJ for financial support (Grant E-26/111.652/2012).

REFERENCES

(1) Totaro, P.; Westrup, K. C. M.; Boulon, M.; Nunes, G. G.; Back, D. F.; Barison, A.; Ciattini, S.; Mannini, M.; Sorace, L.; Soares, J. F.; Cornia, A.; Sessoli, R. *Dalton Trans.* **2013**, *42*, 4416−4426.

(2) Zhu, M.; Li, Y.; Ma, Y.; Li, L.; Liao, D. *Inorg. Chem.* **2013**, *52*, 12326−12328.

(3) (a) Pei, Y.; Journaux, Y.; Dei, A.; Gatteschi, D. *J. Chem. Soc., Chem. Commun.* **1986**, 1300−1301. (b) Pei, Y.; Kahn, O.; Sletten, J. *J. Am. Chem. Soc.* **1986**, *108*, 3143−3145. (c) Kahn, O. *Molecular Magnetism;* VCH: New York, 1993. (d) Kahn, O. *Struct. Bonding (Berlin, Ger.)* **1987**, *68*, 89−167. (e) Kahn, O. *Adv. Inorg. Chem.* **1995**, *43*, 179−259.

(4) Pei, Y.; Verdaguer, M.; Kahn, O.; Sletten, J.; Renard, J.-P. *J. Am. Chem. Soc.* **1986**, *108*, 7428−7430.

(5) (a) Mallah, T.; Thiébaut, S.; Verdaguer, M.; Veillet, P. *Science* **1993**, *262*, 1554−1557. (b) Ferlay, S.; Mallah, T.; Ouahès, R.; Veillet, P.; Verdaguer, M. *Nature* **1995**, *378*, 701−703.

(6) Bencini, A.; Benelli, C.; Caneschi, A.; Carlin, R. L.; Dei, A.; Gatteschi, D. *J. Am. Chem. Soc.* **1985**, *107*, 8128−8136.

(7) (a) Benelli, C.; Gatteschi, D. *Chem. Rev.* **2002**, *102*, 2369−2388. (b) Andruh, M.; Costes, J.-P.; Diaz, C.; Gao, S. *Inorg. Chem.* **2009**, *48*, 3342−3359.

(8) See, for example: (a) Sessoli, R.; Powell, A. K. *Coord. Chem. Rev.* **2009**, *253*, 2328−2341. (b) Aromi, G.; Brechin, E. K. *Struct. Bonding (Berlin, Ger.)* **2006**, *122*, 1−67. (c) Sharples, J. W.; Collison, D. *Coord. Chem. Rev.* **2014**, *260*, 1−216. (d) Woodruff, D. N.; Winpenny, R. E. P.; Layfield, R. A. *Chem. Rev.* **2013**, *113*, 5110−5148. (e) Zhang, P.; Guo, Y.-N.; Tang, J. *Coord. Chem. Rev.* **2013**, *257*, 1728−1763.

(9) See, for example: (a) Coulon, C.; Miyasaka, H.; Clérac, R. *Struct. Bonding (Berlin, Ger.)* **2006**, *122*, 163−206. (b) Sun, H.-L; Wang, Z.-M.; Gao, S. *Coord. Chem. Rev.* **2010**, *254*, 1081−1100. (b) Bernot, K.; Bogani, L.; Caneschi, A.; Gatteschi, D.; Sessoli, R. *J. Am. Chem. Soc.* **2006**, *128*, 7947−7956.

(10) (a) Sorace, L.; Benelli, C.; Gatteschi, D. *Chem. Soc. Rev.* **2011**, *40*, 3092−3104. (b) Nakano, M.; Oshio, H. *Chem. Soc. Rev.* **2011**, *40*, 3239−3248. (c) Rinehart, J. D.; Long, J. R. *Chem. Sci.* **2011**, *2*, 2078−2085.

(11) See for example: (a) Kahn, O.; Larionova, J.; Ouahab, L. *Chem. Commun.* **1999**, 945−952 and references therein. (b) Visinescu, D.; Desplanches, C.; Imaz, I.; Bahers, V.; Pradhan, R.; Villamena, F. A.; Guionneau, P.; Sutter, J.-P. *J. Am. Chem. Soc.* **2006**, *128*, 10202−10212. (c) Novicka, B.; Korzeniak, T.; Stefanczyk, O.; Pincowitz, D.; Chorazy, S.; Sieklucka, B. *Coord. Chem. Rev.* **2012**, *256*, 1946−1971. (d) Sieklucka, B.; Podgajny, R.; Korzeniak, T.; Nowicka, B.; Pincowicz, D.; Koziel, M. *Eur. J. Inorg. Chem.* **2011**, *2011*, 305−326. (e) Wang, X.-Y.; Prosvirin, A.; Dunbar, K. R. *Angew. Chem., Int. Ed.* **2010**, *49*, 5081. (f) Toma, L. M.; Toma, L. D.; Delgado, F. S.; Ruiz-Pérez, C.; Sletten, J.; Cano, J.; Clemente-Juan, J. M.; Lloret, F.; Julve, M. *Coord. Chem. Rev.* **2006**, *250*, 2176−2193.

(12) See, for example: (a) Zhong, Z. J.; Seino, H.; Mizobe, Y.; Hidai, M.; Fujishima, A.; Ohkoshi, S.; Hashimoto, K. *J. Am. Chem. Soc.* **2000**, *122*, 2952−2953. (b) Sieklucka, B.; Podgajny, R.; Przychodzen, P.; Korzeniak, T. *Coord. Chem. Rev.* **2005**, *249*, 2203−2221. (c) Hoeke, V.; Stammler, A.; Bögge, H.; Schnack, J.; Glaser, T. *Inorg. Chem.* **2014**, *53*, 257−268.

(13) (a) Guedes, G. P.; Soriano, S.; Mercante, L. A.; Speziali, N. L.; Novak, M. A.; Andruh, M.; Vaz, M. G. F. *Inorg. Chem.* **2013**, *52*, 8309−8311. (b) Sakamoto, M.; Manseki, K.; Okawa, H. *Coord. Chem. Rev.* **2001**, *219*−*221*, 379−414 and references therein.

(14) See, for example: (a) Le Borgne, T.; Rivière, E.; Marrot, J.; Girerd, J.-J.; Ephritikhine, M. *Angew. Chem., Int. Ed.* **2000**, *39*, 1647−1649. (b) Mishra, A.; Abboud, K. A.; Christou, G. *Inorg. Chem.* **2006**, *45*, 2364−2366.

(15) See, for example: (a) Vaz, M. G. F.; Allão, R. A.; Akpinar, H.; Schlueter, J. A.; Santos, S., Jr.; Lahti, P. M.; Novak, M. A. *Inorg. Chem.* **2012**, *51*, 3138−3145. (b) Dei, A.; Gatteschi, D.; Sangregorio, C.;

Sorace, L. *Acc. Chem. Res.* **2004**, *37*, 827−835. (c) Allão, R. A.; Jordão, A. K.; Resende, J. A. L. C.; Cunha, A. C.; Ferreira, V. F.; Novak, M. A.; Sangregorio, C.; Sorace, L.; Vaz, M. G. F. *Dalton Trans.* **2011**, *40*, 10843−10850. (d) Vaz, M. G. F.; Cassaro, R. A. A.; Akpinar, H.; Schlueter, J. A.; Lahti, P. M.; Novak, M. A. *Chem.—Eur. J.* **2014**, *20*, 5460−5467. (e) Caneschi, A.; Dei, A.; Biani, F. F.; Gutlich, P.; Ksenofontov, V.; Levchenko, G.; Hoefer, A.; Renz, F. *Chem.—Eur. J.* **2001**, *7*, 3926−3930. (f) Vaz, M. G. F.; Akpinar, H.; Guedes, G. P.; Santos Junior, S.; Novak, M. A.; Lahti, P. M. *New J. Chem.* **2013**, *37*, 1927−1932. (g) Fegy, K.; Luneau, D.; Ohm, T.; Paulsen, C.; Rey, P. *Angew. Chem., Int. Ed.* **1998**, *37*, 1270−1273. (h) Kumagai, H.; Inoue, K. *Angew. Chem., Int. Ed.* **1999**, *38*, 1601−1603. (i) Fujita, W.; Awaga, K. *J. Am. Chem. Soc.* **2001**, *123*, 3601−3602. (j) Luneau, D.; Rey, P. *Coord. Chem. Rev.* **2005**, *249*, 2591−2611.

(16) See, for example: (a) Sutter, J.-P.; Kahn, M. L.; Golhen, S.; Ouahab, L.; Kahn, O. *Chem.—Eur. J.* **1998**, *4*, 571−576. (b) Lescop, C.; Luneau, D.; Belorizky, E.; Guillot, M.; Rey, P. *Inorg. Chem.* **1999**, *38*, 5472−5473. (c) Zhao, H.; Bazile, M. J., Jr.; J. Galán−Mascarós, R.; Dunbar, K. R. *Angew. Chem., Int. Ed.* **2003**, *42*, 1015−1018. (d) Sutter, J.-P.; Kahn, M. L. *Magnetism: Molecules to Materials;* Miller, J. S., Drillon, M., Eds.; Wiley-VCH: Weinheim, Germany, 2005; Vol. *5*, p 161.

(17) Yeung, W.-F.; Lau, P.-H.; Lau, T.-C.; Wei, H.-Y.; Sun, H.-L.; Gao, S.; Chen, Z.-D.; Wong, W.-T. *Inorg. Chem.* **2005**, *44*, 6579−6590.

(18) (a) Saber, M. R.; Dunbar, K. R. *Chem. Commun.* **2014**, *50*, 2177−2179. (b) Chelebaeva, E.; Larionova, I.; Guari, Y.; Ferreira, R. A. S.; Carlos, L. D.; Almeida Paz, F. A.; Trifonov, A.; Guérin, C. *Inorg. Chem.* **2009**, *48*, 5983−5995. (c) Ikeda, S.; Hozumi, T.; Hashimoto, K.; Ohkoshi, S. *Dalton Trans.* **2005**, 2120−2123.

(19) (a) Verani, C. N.; Weyhermüller, T.; Rentschler, E.; Bill, E.; Chaudhuri, P. *Chem. Commun.* **1998**, 2475−2476. (b) Verani, C. N.; Rentschler, E.; Weyhermüller, T.; Bill, E.; Chaudhuri, P. *J. Chem. Soc., Dalton Trans.* **2000**, 4263−4271.

(20) Visinescu, D.; Sutter, J.-P.; Ruiz-Pérez, C.; Andruh, M. *Inorg. Chim. Acta* **2006**, *359*, 433−440.

(21) Podgajny, R.; Choeazy, S.; Nitek, W.; Rams, M.; Majcher, A. M.; Marszalek, B.; Żukrowski, J.; Kapusta, C.; Sieklucka, B. *Angew. Chem., Int. Ed.* **2013**, *52*, 896−900.

(22) See, for example: (a) Kou, H.-Z.; Zhou, B. C.; Gao, S.; Wang, R. J. *Angew. Chem., Int. Ed.* **2003**, *42*, 3288. (b) Gheorghe, R.; Andruh, M.; Costes, J.-P.; Donnadieu, B. *Chem. Commun.* **2003**, 2778−2779. (c) Gheorghe, R.; Madalan, A. M.; Costes, J.-P.; Wernsdorfer, W.; Andruh, M. *Dalton Trans.* **2010**, *39*, 4734−4736. (d) Visinescu, D.; Madalan, A. M.; Andruh, M.; Duhayon, C.; Sutter, J.-P.; Ungur, L.; Van den Heuvel, W.; Chibotaru, L. F. *Chem.—Eur. J.* **2009**, *15*, 11808−11814. (e) Sutter, J.-P.; Dhers, S.; Rajamani, R.; Ramasesha, S.; Costes, J.-P.; Duhayon, C.; Vendier, L. *Inorg. Chem.* **2009**, *48*, 5820−5828. (f) Dhers, S.; Feltham, H. L. C.; Clérac, R.; Brooker, S. *Inorg. Chem.* **2013**, *52*, 13685−13691. (g) Alexandru, M.-G.; Visinescu, D.; Madalan, A. M.; Lloret, F.; Julve, M.; Andruh, M. *Inorg. Chem.* **2012**, *51*, 4906−4908. (h) Andruh, M. *Chem. Commun.* **2011**, *47*, 3025−3042 and references therein.

(23) (a) Stumpf, H. O.; Ouahab, L.; Pei, Y.; Grandjean, D.; Kahn, O. *Science* **1993**, *261*, 447−449. (b) Vaz, M. G. F.; Pinheiro, L. M. M.; Stumpf, H. O.; Alcântara, A. F. C.; Gohlen, S.; Ouahab, L.; Cador, O.; Mathonière, C.; Kahn, O. *Chem.—Eur. J.* **1999**, *5*, 1486−1495.

(24) (a) Marvilliers, A.; Pei, Y.; Cano Boquera, J.; Vostrikova, K. E.; Paulsen, C.; Rivière, E.; Audière, J.-P.; Mallah, T. *Chem. Commun.* **1999**, 1951−1952. (b) Vostrikova, K. E.; Luneau, D.; Wernsdorfer, W.; Rey, P.; Verdaguer, M. *J. Am. Chem. Soc.* **2000**, *122*, 718−719. Zhang, Y.-Z.; Li, D.-F.; Clérac, R.; Holmes, S. M. *Polyhedron* **2013**, *64*, 393−398.

(25) (a) Madalan, A. M.; Roesky, H. W.; Andruh, M.; Noltemeyer, M.; Stanica, N. *Chem. Commun.* **2002**, 1638−1639. (b) Zhu, M.; Li, Y.-G.; Ma, Y.; Li, L.-C.; Liao, D.-Z. *Inorg. Chem.* **2013**, *52*, 12326−12328. (c) Zhu, M.; Mei, X.; Ma, Y.; Li, L.; Liao, D.; Sutter, J.-P. *Chem. Commun.* **2014**, *50*, 1906−1908.

(26) Madalan, A. M.; Avarvari, N.; Fourmigué, M.; Clérac, R.; Chibotaru, L. F.; Clima, S.; Andruh, M. *Inorg. Chem.* **2008**, *47*, 940−950.

(27) Zhou, B. H.; Chen, Y. F.; Yin, G. D.; Wu, A. X. *Chin. J. Struct.Chem.* **2006**, *25*, 127−133.

(28) *CrysAlisRED 1.171.32.38;* Oxford Diffraction Ltd.: Abingdon, U.K., 2008.

(29) Sheldrick, G. M. *Acta Crystallogr.* **2008**, *A64*, 112−122.

(30) Larson, A. C. *Crystallogr. Comp. Proc. Int. Summer Sch.* **1970**, 291−294.

(31) Blessing, R. H. *Acta Crystallogr.* **1995**, *A51*, 33−38.

(32) Farrugia, L. J. *J. Appl. Crystallogr.* **1997**, *30*, 565.

(33) Macrae, C. F.; Edginton, P. R.; McCabe, P.; Pidcock, E.; Shields, G. P.; Taylor, R.; Towler, M.; van de Streek, J. *J. Appl. Crystallogr.* **2006**, *39*, 453−457.

(34) Addison, A. W.; Nageswara, T.; Reedijk, J.; van Rijn, J.; Verschoor, G. C. *J. Chem. Soc., Dalton Trans.* **1984**, 1349−1356.

(35) (a) Estes, E. D.; Hatfield, W. E.; Hodgson, D. J. *Inorg. Chem.* **1974**, *13*, 1654−1657. (b) Crawford, V. H.; Richardson, H. W.; Wasson, J. R.; Hodgson, D. J.; Hatfield, W. E. *Inorg. Chem.* **1976**, *15*, 2107−2110. (c) Tuna, F.; Patron, L.; Journaux, Y.; Andruh, M.; Plass, W.; Trombe, J.-C. *J. Chem. Soc., Dalton Trans.* **1999**, 539−546. (d) Ruiz, E.; Rodriguez-Fortera, A.; Alemany, P.; Alvarez, S. *Polyhedron* **2001**, *20*, 1323−1330.

(36) Azuah, R. T.; Kneller, L. R.; Qiu, Y.; Tregenna-Piggott, P. L. W.; Brown, C. M.; Copley, J. R. D.; Dimeo, R. M. *J. Res. Natl. Inst. Stan. Technol.* **2009**, *114*, 341−358.

(37) (a) Oshio, H. *Inorg. Chim. Acta* **2001**, *324*, 188−193. (b) Zhang, L.; Li, S.-Q.; Sun, B.-W.; Liao, D.-Z.; Jiang, Z.-H.; Yan, S.-P.; Wang, G.-L.; Yao, X.-K.; Wang, H.-G. *Polyhedron* **1999**, *18*, 781−785. (c) Bencini, A., Gatteschi, D. *EPR of Exchange Coupled Systems;* Springer-Verlag: Berlin, 1990.

(38) (a) Costes, J. P.; Dahan, F.; Nicodeme, F. *Inorg.Chem.* **2001**, *40*, 5285−5287. (b) Guo, F.-S.; Leng, J.-D.; Liu, J.-L.; Meng, Z.-S.; Tong, M.-L. *Inorg. Chem.* **2012**, *51*, 405−413.

(39) See, for example: (a) Luo, F.; Che, Y.-X.; Zheng, J.-M. *Cryst. Growth Des.* **2006**, *6*, 2432−2434. (b) Sopasis, G. J.; Canaj, A. B.; Phillipidis, A.; Siczek, M.; Lis, T.; O'Brien, J. R.; Antonakis, M. M.; Pergantis, S. A.; Milios, C. J. *Inorg. Chem.* **2102**, *51*, 5911−5918. (c) Chandrasehkar, V.; Dey, A.; Das, S.; Rouzières, M.; Clérac, R. *Inorg. Chem.* **2013**, *52*, 2588−2598. (d) Guo, F.-S.; Chen, Y.-C.; Liu, J.-L.; Leng, J.-D.; Meng, Z.-S.; Vrábel, P.; Orendáč, M.; Tong, M. L. *Chem. Commun.* **2012**, *48*, 12219−12221. (e) Li, Z.-Y.; Xin, G.; Zhang, J.-J.; Huang, H.-Q.; Duan, C.-Y. *Cryst. Growth Des.* **2013**, *13*, 3429−3437. (f) Zhu, Q.; Xiang, S.; Sheng, T.; Yuan, D.; Shen, C.; Tan, C.; Hu, S.; Wu, X. *Chem. Commun.* **2012**, *48*, 10736−10738. (g) Zhang, H.; Zhuang, C.-L.; Kong, X.-J.; Ren, Y.-P.; Long, L.-S.; Huang, R.-B.; Zheng, L.-S. *Cryst. Growth Des.* **2013**, *13*, 2493−2498.

(40) Murakami, R.; Nakamura, T.; Ishida, T. *Dalton Trans.* **2014**, *43*, 5893−5898.

(41) (a) Ishida, T.; Murakami, R.; Kanetomo, T.; Nojiri, H. *Polyhedron* **2013**, *66*, 183−187. (b) Kanetomo, T.; Ishida, T. *Chem. Commun.* **2014**, *50*, 2529−2531.

(42) Novak, M. A. *J. Magn. Magn. Mater.* **2004**, *E707*, 272−276.

(43) Mydosh, J. *Spin Glasses: An Experimental Introduction;* Taylor and Francis: London, U.K., 1993.

(44) (a) Cole, K. S.; Cole, R. H. *J. Chem. Phys.* **1941**, *9*, 341−352. (b) Costes, M.; Broto, J. M.; Raquet, B.; Rakoto, H.; Novak, M. A.; Sinnecker, J. P.; Soriano, S.; Folly, W. S. D.; Maignan, A.; Hardy, V. *J. Magn. Magn. Mater.* **2005**, *294*, E123−E126.